In Vivo Imaging and Toxicity Assessments of Fluorescent Nanodiamonds inCaenorhabditis elegans

ARTICLE *in* NANO LETTERS · SEPTEMBER 2010

Impact Factor: 13.59 · DOI: 10.1021/nl1021909 · Source: PubMed

5 AUTHORS, INCLUDING:

Nitin Mohan
Ecole normale supérieure de Cachan
7 PUBLICATIONS **242** CITATIONS
SEE PROFILE

Yi-Chun Wu
National Taiwan University
33 PUBLICATIONS **2,130** CITATIONS
SEE PROFILE

NANO LETTERS

pubs.acs.org/NanoLett

In Vivo Imaging and Toxicity Assessments of Fluorescent Nanodiamonds in *Caenorhabditis elegans*

Nitin Mohan,[†,‡,§] Chao-Sheng Chen,[‡] Hsiao-Han Hsieh,[||] Yi-Chun Wu,[*,||] and Huan-Cheng Chang[*,‡,§]

[†]Department of Engineering and System Science, National Tsing Hua University, Hsinchu 300, Taiwan, [‡]Institute of Atomic and Molecular Sciences, Academia Sinica, Taipei 106, Taiwan, [§]Nano Science and Technology Program, Taiwan International Graduate Program, Institute of Physics, Academia Sinica, Taipei 115, Taiwan, and [||]Institute of Molecular and Cellular Biology, National Taiwan University, Taipei 106, Taiwan

ABSTRACT Nanoscale carbon materials hold great promise for biotechnological and biomedical applications. Fluorescent nanodiamond (FND) is a recent new addition to members of the nanocarbon family. Here, we report long-term in vivo imaging of FNDs in *Caenorhabditis elegans* (*C. elegans*) and explore the nano-biointeractions between this novel nanomaterial and the model organism. FNDs are introduced into wild-type *C. elegans* by either feeding them with colloidal FND solution or microinjecting FND suspension into the gonads of the worms. On feeding, bare FNDs stay in the intestinal lumen, while FNDs conjugated with biomolecules (such as dextran and bovine serum albumin) are absorbed into the intestinal cells. On microinjection, FNDs are dispersed in the gonad and delivered to the embryos and eventually into the hatched larvae in the next generation. The toxicity assessments, performed by employing longevity and reproductive potential as physiological indicators and measuring stress responses with use of reporter genes, show that FNDs are stable and nontoxic and do not cause any detectable stress to the worms. The high brightness, excellent photostability, and nontoxic nature of the nanomaterial have enabled continuous imaging of the whole digestive system and tracking of the cellular and developmental processes of the living organism for several days.

KEYWORDS Bioimaging, *C. elegans*, fluorescent nanodiamonds, in vivo toxicity, stress responses

Optical imaging is an ideal noninvasive tool to visualize biological processes, right at molecular and cellular levels, by probing specific biomolecules and their intermolecular interactions. In vivo imaging, in particular, enables the study of molecular dynamics in both real time and three dimensions without perturbing the whole systems externally. Recent advances in the development of fluorescent nanoparticles and their applications in life sciences have complemented nanotechnology with advanced imaging technology.[1] For example, several nanoparticles including quantum dots,[2] up-conversion phosphors,[3] and silicon[4] and carbon[5,6] nanoparticles have been used as biomarkers. Among them, fluorescent nanodiamond (FND) has drawn much attention in recent years as a promising fluorescent nanoprobe for bioimaging applications.[7−12] The material contains negatively charged nitrogen-vacancy centers, $(N-V)^-$, as fluorophores. Unique photophysical features such as extended far-red emission (600−800 nm), long fluorescence lifetimes (~10 ns), and excellent photostability (i.e., no photobleaching and no photoblinking), along with the easiness in surface functionalization of the carbon-based nanomaterial, have made FND a potential candidate for long-term imaging in vivo. While FND, or nanodiamonds in general, has been demonstrated by a number of research groups[7,13−17] to be biocompatible and nontoxic to cells, systematic in-depth studies of the toxicity induced by the nanoparticles in whole organisms have not yet been performed. Such knowledge is imperative for its future biological and biomedical applications. Here, we report an in vivo study of FNDs in the model organism *Caenorhabditis elegans* (*C. elegans*).

C. elegans is a free living soil nematode with simple and well-defined anatomy. The 1 mm long adult hermaphrodite consists of an invariable number of 959 cells, which are organized to form complex tissues including intestine, muscle, hypodermis, gonad, and nerve systems.[18,19] The genome of *C. elegans* has been completely sequenced,[20] making it feasible to study biological processes at the molecular level. The worm has also been employed as a benchmark system for ecotoxicological studies owing to its short life cycles, ease in handling, and high sensitivity to various types of stresses.[21,22] Moreover, its body is optically transparent. This allows in vivo imaging of the whole organism as well as in situ determination of the biodistribution of the internalized fluorescent nanoparticles and assessment of their toxic effects at the same time, which could otherwise be difficult with opaque animal models like mouse.[23,24]

* To whom correspondence may be addressed, yichun@ntu.edu.tw or hchang@gate.sinica.edu.tw.

Received for review: 6/22/2010
Published on Web: 00/00/0000

DOI: 10.1021/nl1021909 | *Nano Lett.* **XXXX,** *xxx,* 000–000

A prior study has used fluorescent nanoparticles for in vivo imaging of *C. elegans*. Austin and co-workers[3] showed that the up-conversion phosphors composed of Y_2O_3:Yb,Er (size of 50−200 nm) can be imaged in the digestive system using a fluorescence microscope and a near-infrared laser as the light source. The phosphors, after uptake by the worms, were visible in the intestines with most of the particles found beyond pharynx and extending to rectum. The authors also checked the survival rate of the organism over a period of 6 h and discovered little acute toxic effects of the material.[25] In contrast, serious reproductive senescence and early death of the organism were found for nanoparticles made of silver[26] and silica.[27]

This work demonstrates that FND is an innovative fluorescent marker for in vivo imaging applications. In addition, we integrate physiological indicators (such as life span and progeny production) with sensitive stress biomarkers (such as stress-response gene expression and protein localization) to assess the toxicity and stress response induced by bare or bioconjugated FNDs to the living organism. Our results indicate that this carbon-based nanomaterial has neither detectable in vivo toxicity nor any apparent side effects, like stress response.

Results and Discussion. Figure 1A displays an epifluorescence and differential interference contrast (DIC) merged image of a typical wild-type *C. elegans* hermaphrodite. The worm was grown at 20 °C in the nematode growth medium (NGM) seeded with *Escherichia coli* (*E. coli*). Prior to optical imaging, the worm was transferred onto an agar pad, anesthetized, and then sealed with a coverslip. When excited with green-yellow light, the wild-type worms showed very weak background signals at $\lambda_{em} > 600$ nm as the autofluorescence resulting from the excitation can be efficiently blocked by using appropriate excitation/emission filter sets (see Methods and Materials section). However, as bare FNDs (∼120 nm in diameter) were incorporated into the worms by feeding in the absence of *E. coli*, bright red fluorescence was easily visible in the lumen of the digestive system, extending from the pharynx to the anal region (Figure 1B). It indicates that FNDs were not regarded by the worms as repellents during the feeding process. Interestingly, the particles were retained in the lumen even after 12 h of feeding (Figure 1C). Such retention may be caused, at least in part, by slow or no FND excretion since it has been shown that the excretion of nanoparticles such as Y_2O_3:Yb,Er is inhibited when the worms are deprived of food.[3] The persistence of FNDs in the gut of the treated worms reflects that the nanomaterial is biostable and is resistant to the worm's robust digestive enzymes, which can degrade intestinal bacteria in less than 2 min.[28] It should be noted that there is no translocation of FNDs into the intestinal cells. This could be because the bare FND particles formed large aggregates inside the intestinal lumen, preventing them from entering the cells. Alternatively, the FNDs may have not been recognized and taken up by the active transport

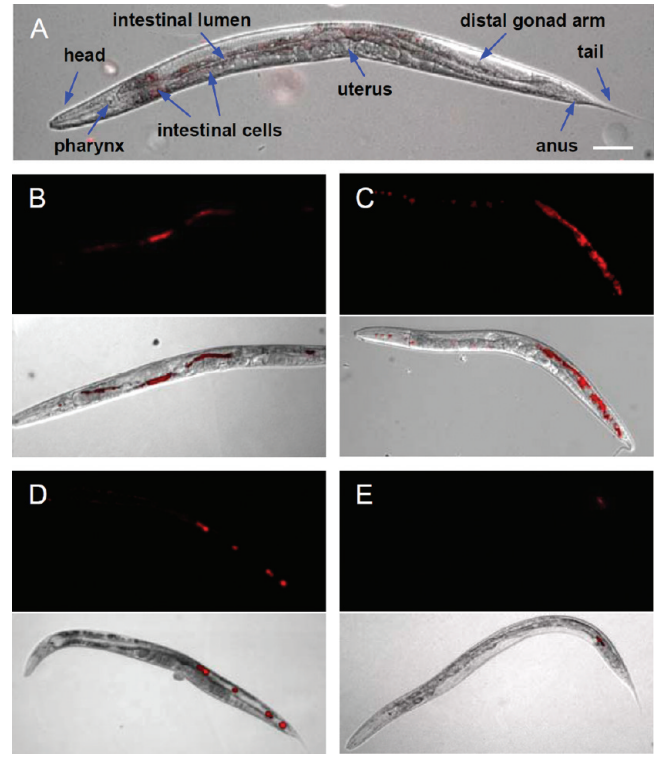

FIGURE 1. Epifluorescence and epifluorescence/DIC-merged images of wild-type *C. elegans*. (A) An untreated young adult. (B, C) Worms fed with bare FNDs for 2 h (B) and 12 h (C). The FNDs stayed inside the gut and were not excreted out when the worms were deprived of food. Excretion of FNDs occurred upon feeding with *E. coli*. (D, E) Worms were provided with *E. coli* for 20 min (D) and 40 min (E), after being fed with bare FNDs for 2 h. Almost, if not all, FNDs were excreted out within 1 h. The upper panels in (B−E) show the epifluorescence images; (A) and the lower panels in (B−E) show the epifluorescence/DIC-merged images. Anterior is left and dorsal is up in all figures. Scale bar is 50 μm.

system of the intestinal cells. By collecting ∼600 worms and digesting them in strong acids (see Materials and Methods), we determined from fluorescence intensity measurements that the amount of FNDs in the intestinal lumen after being fed with the particles for 2 h was in the range of ∼3 ng/worm or $\sim 1 \times 10^6$ particles/worm.

Upon resumption of feeding the worms with *E. coli*, the FNDs were pushed down through the gut lumen and were excreted out within an hour. We imaged the worms at 20 min (Figure 1D) and 40 min (Figure 1E) after their recovery on food to track the movement of FNDs through their digestive tracts. It is found that the worms display a normal feeding behavior as those worms without the FND treatment, suggesting that exposure to and consumption of FNDs do not cause a gross behavior defect. To examine the photostability of the FNDs in vivo, we imaged the entire digestive tract of the worm for more than 48 h and found that there is neither photobleaching nor photoblinking of the nanomaterial in the lumen. A movie showing freely moving *C. elegans* with FNDs inside the gut and the ejection of FNDs after being fed with bacteria can be found in the Supporting Information.

DOI: 10.1021/nl1021909 | *Nano Lett.* **XXXX,** *xxx,* 000–000

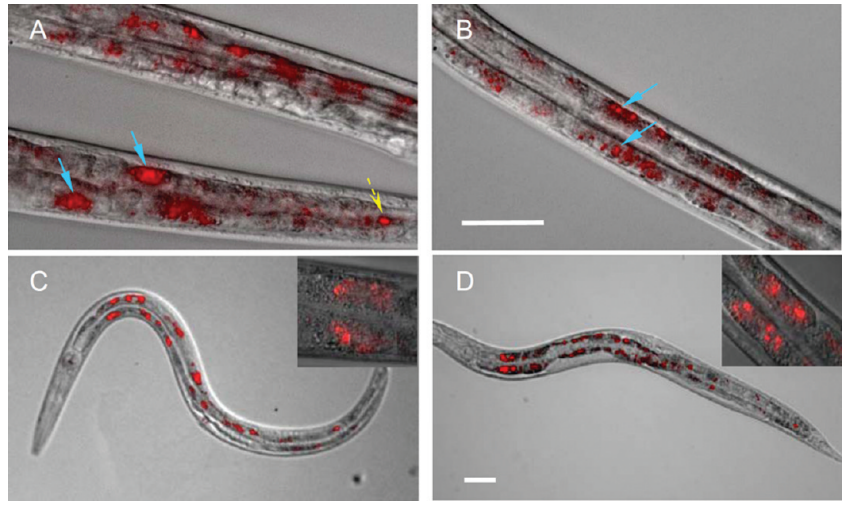

FIGURE 2. Epifluorescence/DIC-merged images of wild-type *C. elegans* fed with bioconjugated FNDs. (A, B) Worms fed with dextran-coated FNDs (A) and BSA-coated FNDs (B) for 3 h. FNDs can be seen to be localized within in the intestinal cells (blue solid arrows) and a few stay in the lumen (yellow dash arrow). (C, D) Worms fed with dextran-coated (C) and BSA-coated (D) FNDs for 3 h and recovered on to *E. coli* bacterial lawns for 1 h. In both cases, the FNDs staying in the lumen are excreted out, whereas the ones localized in the cells retain. Insets: 100× magnified images of the FNDs within the intestinal cells. Anterior is left and dorsal is up in all the figures. Scale bars are 50 μm.

FND is composed of sp^3 carbon. Its surface can be readily grafted with carboxyl groups for ensuing conjugation with biomolecules such as carbohydrates, proteins, and nucleic acids based on carbodiimide chemistry.[8,15,29,30] Starting with carboxylated FNDs prepared by oxidative acid treatment,[29] we conjugated them covalently with carboxymethyldextran (CMDx) and bovine serum albumin (BSA). The bioconjugated FNDs were then orally administered into the worms by the same procedures as before. Strikingly, we found that most of the dextran- and BSA-coated FNDs are absorbed into the intestinal cells, with very few still remaining in the gut lumen region (panels A and B of Figure 2). As the worms were transferred to the bacterial lawn for recovery for an hour, the residual FNDs within the gut lumen were excreted out, whereas the FND bioconjugates absorbed into the cells retained (panels C and D of Figure 2). We observed that the FND bioconjugates stayed within the cells even after recovery on bacteria for 24 h. It is likely that the surface modifications made FNDs disperse better in the solution, prevented their aggregation inside the gut, and thus helped their uptake via endocytosis by the intestinal cells.[28,31] Additionally, the bioconjugation could have activated some receptor-mediated endocytosis pathway(s), which facilitated FNDs to be absorbed into the intestinal cells from the lumen. The absorption process is more or less uniform throughout the whole intestinal tract, with slightly more absorption in the anterior than that in the posterior cells. Insets in panels C and D of Figure 2 show enlarged views of the localization of FNDs in the intestinal cells (see also Figure S1 in Supporting Information for serial *z*-section images). Similar results are obtained for ~40 nm FND particles (cf. Figure S2 in Supporting Information).

Feeding is a passive way of incorporating FNDs into *C. elegans*. Microinjection serves as an alternative to actively introduce FNDs to specific locations in the worms. More interestingly, FNDs can be delivered to the next generation if the particles are injected to the gonad of an adult hermaphrodite. In this experiment, a well-dispersed solution of bare FNDs was microinjected into the distal gonads of gravid hermaphrodites.[32] The injected worms were then transferred to bacterial lawns (see Materials and Methods for details). Figure 3A shows the injection site and how the injected FNDs are dispersed in the germline syncytium, where the germline nuclei share the same cytoplasm. The FNDs were observed to be incorporated into oocytes during oogenesis[33] within 30 min after the injection. Furthermore, they retained in the fertilized zygotes and their fluorescence signals persisted throughout embryogenesis (panels B and C of Figure 3). Most importantly, there is no indication that the FNDs caused any abnormal embryonic development such as intracorporal hatching of eggs in the parent worms as observed for silica nanoparticles.[27] The observations again assert that FND is nontoxic to the organism. Notably, the FND particles are localized to the cytoplasm of many cells in the early embryos (Figure 3B) but predominantly to the intestines of the late embryos (Figure 3C).

Thus we have successfully introduced FNDs into the cells (i.e., intestinal and embryonic cells) of *C. elegans* with no apparent deleterious effects on its growth and development. Next, we investigate in greater detail the toxicity of the FNDs absorbed into the intestinal cells of hermaphrodites. We first used life span and reproductive potential as indicators for our toxicity studies. Specifically, we performed life span and brood size assays for worms treated with or without bioconjugated FNDs (both dextran- and BSA-coated) and compared the results. As shown in parts A and B of Figure 4, the FND-treated (or FND-tagged) worms appear normal and have no deviation from the untreated controls in both

DOI: 10.1021/nl1021909 | *Nano Lett.* **XXXX,** *xxx,* 000–000

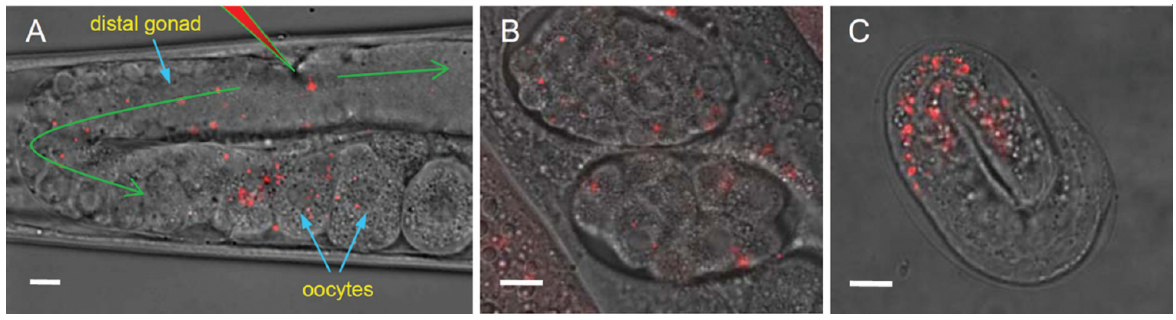

FIGURE 3. Microinjection of bare FNDs into *C. elegans*. (A−C) Epifluorescence/DIC-merged images of an injected worm (A) and its progeny at the early (B) and late (C) embryonic stages. The FNDs dispersed in the distal gonad and oocytes at approximately 30 min after injection (A). Green arrows indicate bulk streaming of FNDs with cytoplasmic materials and the red triangle indicates the site of injection. Note that the injected FNDs are present in the cytoplasm of many cells in the early embryos (B) but predominantly in the intestinal cells of the late embryo (C). Scale bars are 10 μm.

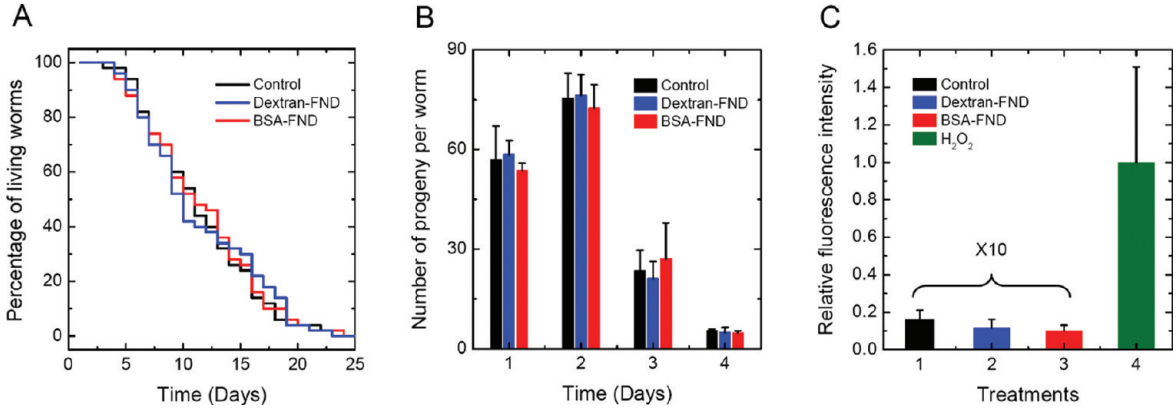

FIGURE 4. Life span, brood size, and ROS assays for *C. elegans*. (A−C) Comparisons of life span (A), brood size (B), and ROS level (C) of the worms treated with bioconjugated FNDs, and the untreated controls show that both the life span and the potential for progeny production are unaffected by the treatments with either dextran- or BSA-coated FNDs. In (C), a hydrogen peroxide treatment was used as the positive control for the ROS assay. Note that the data of the untreated control and the FND treatments were magnified 10-fold for clarity.

longevity and progeny production. The inertness of the material stands as a sharp contrast to previous findings for silver nanoparticles,[26] which can cause early death of the organism.

In *C. elegans*, the brood size and longevity have been shown to be affected by the level of reactive oxygen species (ROS) accumulated in the cells.[34,35] Since no detectable change was found in either brood size or longevity of the animal treated with FNDs, it implies that the particles do not significantly affect the ROS level in both germline and somatic cells. To further confirm this assessment, we conducted a direct ROS measurement and explored the stress response of the organism to FND at the molecular level.[36] The amount of ROS was determined by the hydrolysis of a fluorescent ROS detection reagent, CM-H_2DCFDA (see Methods and Materials and Figure S3 in Supporting Information for fluorescence images). As shown in Figure 4C, the relative ROS amount of the worms treated with FNDs is essentially the same as that of the untreated control, indicating that FND does not induce ROS generation in *C. elegans*. A similar observation of no increase of the ROS level was made for nonfluorescent nanodiamonds in neuroblastoma cells.[14]

C. elegans is a powerful model for the study of innate immunity and stress response, and its intestine is a major site responsive to toxins and chemical stressors in the environment.[37] Despite the fact that the worm does not have homologues of TRAF or NFkB, which are important for human innate immunity, it has the conserved stress-response pathways mediated by DAF-16/FOXO and SKN-1 that allow us to study the effect of the FND treatment on these two major stress-response pathways.[38] In the following, we examined the activities of two major stress-response pathways mediated by the genes *daf-16* and *skn-1* in the control and FND-treated worms to assess the stress that may be induced by FNDs to the whole organism. Heat-shock and arsenic treatments were used as positive controls to elicit the stress responses in our assays.

In mammals and nematodes, activation of the DAF-16/FOXO transcription factor results in resistance to some types of stress.[38] Under the optimal growth condition, the DAF-16 protein is primarily localized to the cytoplasm; when exposed to oxidative or thermal stress, DAF-16 is translocated to the nucleus where it regulates the expression of a set of genes including antioxidant genes (such as catalase

DOI: 10.1021/nl1021909 | *Nano Lett.* **XXXX,** *xxx,* 000−000

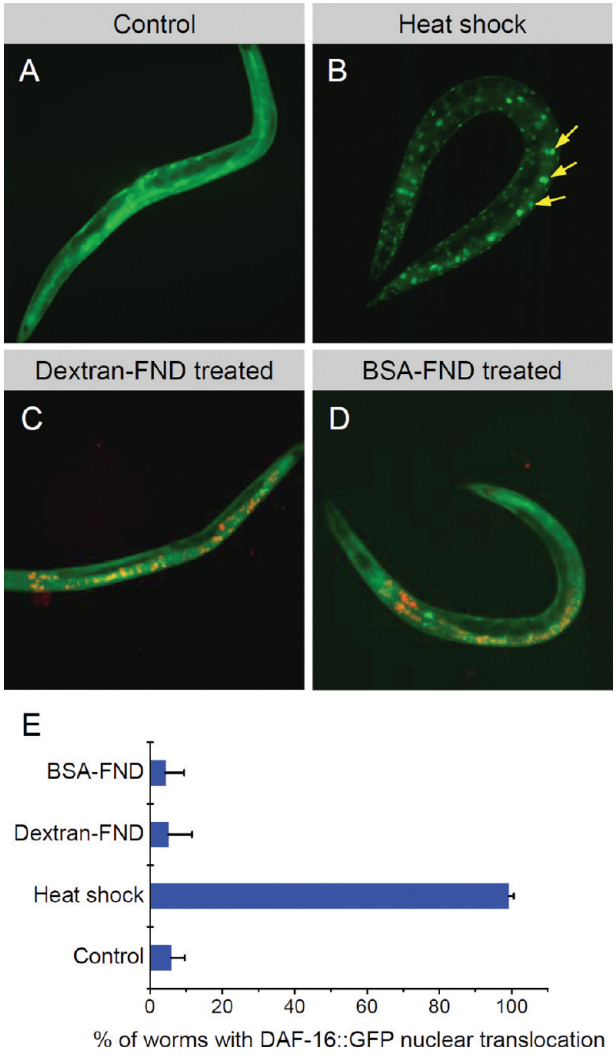

FIGURE 5. Stress-response assays by nuclear translocation of DAF-16::GFP in *C. elegans*. (A−D) Epifluorescence images of the control (A), heat-shocked (B), and FND-treated (C, D) worms. The green and red fluorescence signals are from GFPs and FNDs, respectively. Under normal conditions, DAF-16::GFP was mostly distributed in the cytoplasm of the cells (A), whereas the protein was translocated into the nuclei after heat shock (yellow arrows in B). When the worms were treated with dextran-coated FNDs (C) or BSA-coated FNDs (D), their DAF-16::GFP localization patterns were similar to that of (A) and were not predominantly nuclear. (E) A quantitative analysis, showing that no significant stress response is caused by the dextran- or BSA-coated FND treatment. Approximately 120 worms were observed in each case.

and Mn-superoxide dismutase), chaperones, and antimicrobial and metabolic genes to increase stress tolerance.[39] We utilized the transgenic worms bearing the *daf-16::gfp* construct (see Materials and Methods), where a green fluorescent protein (GFP) is fused to the C terminus of DAF-16,[40] as a stress response reporter. Figure 5 shows overlaid images from the GFP fluorescence channel (green) and the FND fluorescence channel (red) of the control and the treated worms. As seen, DAF-16::GFP was primarily distributed in the cytoplasm under the normal physiological condition (Figure 5A), but the cytoplasmic DAF-16::GFP was translocated into the nuclei of the intestinal cells under heat shock (Figure 5B). In contrast to the heat-shock treatment, the bioconjugated FNDs did not cause any significant nuclear translocation of the cytoplasmic DAF-16::GFP (panels C and D of Figure 5 for dextran- and BSA-coated FND treatments, respectively). A quantitative analysis with ∼120 worms supports the assessment (Figure 5E). To further confirm that the lack of the stress response to the FNDs is not because the FND-treated worms fail to respond to the stress due to the deleterious effect caused by the nanomaterial but, instead, because the worms do not regard FNDs as stressors, we heat-shocked worms that had been previously fed with bioconjugated FNDs. After the heat-shock treatment, the DAF-16::GFP proteins became predominantly localized to the nuclei (see Figure S4 in Supporting Information), showing responsiveness to the heat-shock stress in the FND-containing worms. This result verifies that the function of the stress response genes is not hindered by the FND treatment.

Apart from DAF-16, the transcription factor SKN-1 also regulates a bank of genes that detoxify and protect the organism against reactive oxygen species and environmental toxins.[41] One of the best characterized target genes of SKN-1 is *gcs-1*. The gene encodes γ-glutamine cysteine synthetase heavy chain, which is rate limiting for glutathione synthesis and is expressed in the intestine in a stress-inducible manner.[41] We used the transgenic strain bearing the fusion construct *gcs-1::gfp*, in which *gfp* is expressed under the control of the *gcs-1* promoter,[41] to assess the SKN-1 transcriptional activity in the presence of FND. As shown in Figure 6A, the GFP was expressed in the pharynx, nearby neurons, and anterior and posterior intestine under the normal physiological conditions. When the transgenic worms were exposed to the arsenic solution, the content of their intestinal GFPs increased dramatically (Figure 6B). The treatment with bioconjugated FNDs (panels C and D in Figure 6), on the other hand, did not significantly increase the GFP expression level of the *gcs-1::gfp* transgene in the intestine, as compared to that of the wild type (Figure 6E). We have also performed the stress response experiments at different time points, which all yielded similar results. For example, the organism did not show any detectable stress response even after being fed with the FND bioconjugates for 6 h and allowed to recover for 1 h. These results in combination with the aforementioned stress-response studies using the *daf-16::gfp* reporter provide strong evidence that FND is biologically inert and does not cause significant stress to the organism.

Conclusion and Summary. We have used feeding and microinjection methods to deliver FNDs into *C. elegans* and successfully performed multiple sensitive assays to study the interaction between the nanoparticles and the host organism. Through feeding, we found that bare FNDs were stuck within the lumen, whereas bioconjugated FNDs were absorbed into the intestinal cells, likely by endocytosis. The

DOI: 10.1021/nl1021909 | *Nano Lett.* **XXXX,** *xxx,* 000–000

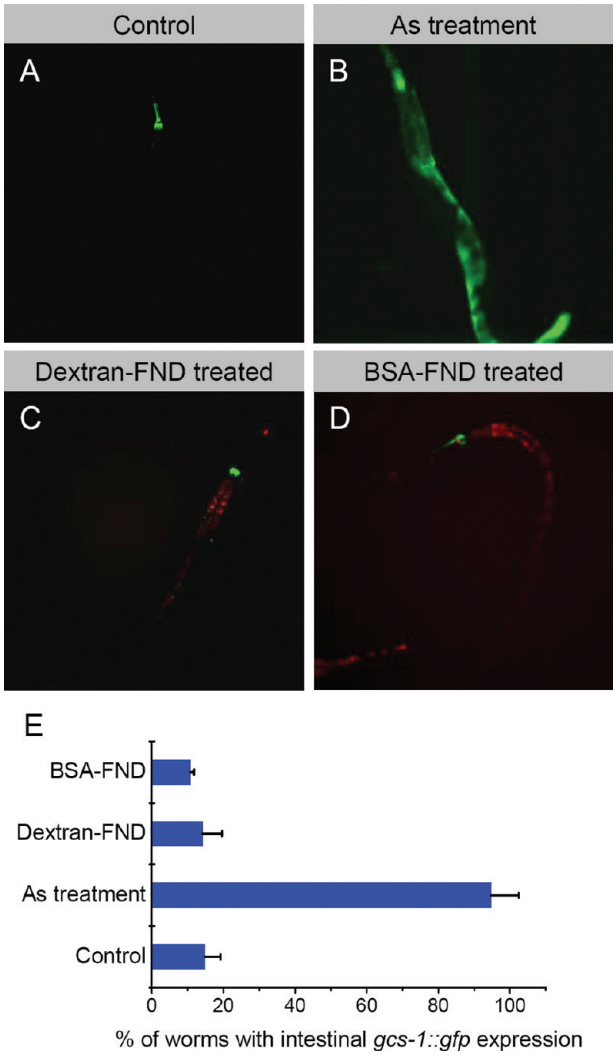

FIGURE 6. Stress-response assays by nuclear *gcs-1::gfp* expression in *C. elegans*. (A−D) Epifluorescence images of worms carrying the *gcs-1::gfp* transgenes under normal conditions (A), treatment in arsenic solution (B), and treatments with bioconjugated FNDs (C, D). The green and red fluorescence signals are from GFPs and FNDs, respectively. GFP expression was observed only in the pharynx and nearby cells in the control worm under normal conditions (A), whereas the expression in the intestine dramatically increased after the arsenic treatment (B). When the worms were treated with dextran-coated FNDs (C) or BSA-coated FNDs (D), the GFP expression patterns shared close similarities with that of (A). (E) A quantitative analysis showing insignificant difference between worms under normal conditions or with the FND treatments. Approximately 120 worms were observed in each case.

absorbed FNDs remained within the cells even after feeding the worms with bacteria. Life span, brood size, and ROS measurements proved that the presence of FNDs in the cells does not cause any change in longevity and reproductive potential of the organism. Moreover, the assays using different stress-response genes (*daf-16* and *gcs-1*) showed that the FNDs do not induce any detectable stress to the organism. These findings altogether confirm that FND is biocompatible and nontoxic, supporting the suggestion that the material is an ideal fluorescent nanoprobe for long-term in vivo imaging. It may serve as a useful tool to fluorescently tag living whole organisms too.

In addition to feeding the worms with FNDs, we microinjected FNDs into the gonads of adult hermaphrodites, and the particles were subsequently delivered to their embryos. This procedure allows us to successfully incorporate FNDs into the second generation of the organism. The entire embryonic development of the FND-containing embryos has been followed and appears to be normal. The observation indicates that FND is biologically inert, it does not cause any abnormality in cell division, differentiation, or morphogenesis during embryogenesis, and it does not elicit any detectable stress response. Since cell division, differentiation, and morphogenesis are critical to the development and health of multicellular organisms and many genes involved in these cellular processes and in the stress-response pathways have been shown to be evolutionarily conserved from *C. elegans* to humans, our findings in *C. elegans* could have important implications in other species. With the excellent photophysical properties and the nontoxic nature of the novel nanomaterial, FND is expected to become one of the most prominent fluorescent nanoprobes for long-term tracking and imaging of cellular and developmental processes of live animals.

Materials and Methods. ***Materials and Chemicals.*** Synthetic type Ib diamond powders (Micron+ MDA 0−0.01 μm), typically containing 100 ppm of atomic nitrogen, were obtained from Element Six. All chemicals used in this work were obtained from commercial sources and used without further purification.

FND Production. Diamond powders were radiation-damaged by 40 keV He^+ bombardment to create vacancies within their crystal lattices.[11,42] Predominantly $(N-V)^-$ centers were formed upon annealing the irradiated nanocrystallites at 800 °C for 2 h. To remove graphitic surface structures induced by the ion irradiation as well as the thermal annealing, the freshly prepared FNDs were oxidized at 450 °C for 1 h, cleaned in concentrated H_2SO_4−HNO_3 (3:1, v/v) solution at 100 °C for 3 h, separated by centrifugation, and finally rinsed extensively in deionized water. Dynamic light scattering measurements with a particle analyzer (Delsa Nano C, Beckman-Coulter) indicated an average size of ∼120 nm (see Figure S5 in Supporting Information).

Bioconjugation. Dextran coating was conducted by dispersing the acid-treated FNDs (10 mg) in water (10 mL) containing *N*-ethyl-*N*′-(3-(dimethylamino)propyl)carbodiimide (EDC, 10 mg) and *N*-hydroxysuccinimide (NHS, 8 mg) to activate surface carboxyl groups. After 30 min, the activated FNDs were separated by centrifugation, resuspended in phosphate buffer saline (10 mL), and reacted with poly-L-lysine (10 mg) for 3 h for surface grafting with amino groups. To conjugate with dextran, the amine-grafted FNDs were mixed with CMDx (0.013 M, 10 mL) and activated with EDC (25 mg) and NHS (15 mg). The conjugation reaction proceeded for 36 h at room temperature. Similar procedures

DOI: 10.1021/nl1021909 | *Nano Lett.* **XXXX,** *xxx,* 000–000

applied to covalent conjugation of BSA (6 mg) with FNDs. The average sizes of the dextran- and BSA-coated FND particles were ~290 and ~170 nm, respectively (see Figure S5 in Supporting Information).

Worm Strains and Culture. The Bristol N2 (wild type) strain and transgenic strains bearing *daf-16::gfp* and *gcs-1::gfp* reporter constructs were grown on NGM agar plates at 20 °C, except where otherwise noted. The worms were fed with *E. coli* strain OP50 according to standard protocol.[43]

Feeding. Approximately 15−20 young adults or L4 stage of growing hermaphrodites were picked onto NGM plates not seeded with *E. coli*. An aliquot (300 μL) of either bare or bioconjugated FND solution (1 mg/mL) was dropped on the plate. The worms were incubated with the FNDs for 2−3 h at 20 °C, after which they were recovered onto bacteria-seeded NGM plates for 1 h.

Microinjection. Needles (World Precision Instruments) pulled by a vertical micropipet puller (Sutter Instruments) were filled with bare FND suspension (0.5 mg/mL), which had been ultrasonicated for 1 h at room temperature. The needles were mounted on a microinjector controlled by a micromanipulator (model 5170, Eppendorf) fixed on an inverted microscope (Axiovert 10, Zeiss). The worms were injected by standard procedures as described in ref 32.

Imaging. Young adult worms were picked onto an agar pad that was afterward sandwiched between two coverslips. Sodium azide or levamisole (Sigma) was added to immobilize the worms. An inverted fluorescence microscope (TE 2000, Nikon) equipped with an electron multiplying CCD camera (iXon, Andor) acquired images of the worms with FNDs at both DIC and wide-field epifluorescence geometries. Two DIC microscope objectives, 20× DIC M, 0.5 NA (Plan Fluor), and 60× DIC H, 1.4 NA (Plan Apo), were used for imaging at different magnifications. FNDs were excited with a mercury lamp (λ_{ex} = 510−560 nm), and the resulting emission was collected above 600 nm using a long-pass filter. GFPs were imaged under excitation at λ_{ex} = 450−490 nm and the emission was observed above 520 nm. All the images were processed by Image Pro Plus.

Brood Size and Life Span Assays. Wild-type L4 larvae were fed with bioconjugated FNDs for 3 h and were transferred onto bacteria-seeded NGM plates for recovery. The worms were subsequently transferred onto a new bacteria plate every day, and the number of newly hatched larvae was counted. This was repeated for 4 days until the mother worms stopped laying eggs. Each day the progeny production was recorded and was compared with the untreated controls. The same procedures of feeding FNDs were followed for the life span measurements, and we observed for how long the worms survived. Everyday, the worms were transferred to a new *E. coli* plate and confirmed that they were alive by observing their movement on the plate. In both assays, we observed 20 worms at a time and repeated the experiments five times.

ROS Measurement. Wild-type young adult worms were fed with bioconjugated FNDs for 3 h and were transferred onto bacteria-seeded NGM plates for recovery. Worms were then transferred to Hank's solution (300 μL) containing 10 μM CM-H_2DCFDA (Invitrogen) and incubated for 2 h at 25 °C.[36] To observe the fluorescence of the ROS detection reagent, the samples were imaged as described before with excitation at λ_{ex} = 450−490 nm and emission collected above 520 nm. The fluorescence of the whole body was determined by using home-built Labview 9.0 software that summed up the intensity counts from all pixels in the frame, above a threshold set to eliminate background signals. For the positive control, young adult worms were treated with 10 mM H_2O_2 for 5 h at 25 °C prior to the ROS measurement. Approximately 20 worms were observed in each case.

Stress Responses Assays. The transgenic strains bearing either the *daf-16::gfp* or *gcs-1::gfp* reporter construct were fed with bioconjugated FNDs for 3 h. They were recovered onto a bacterial lawn for 1 h prior to stress responses assays. In heat shock experiments, the *daf-16::gfp* transgenic worms on the bacteria-seeded plate were immersed in a water bath at 34 °C for 3 h and were recovered for 4 h at 20 °C before observation. The arsenic treatment was performed as previously described.[44] In brief, the *gcs-1::gfp* worms were treated with 1 mM As(III) solution for 3 h and were recovered for 1 h on plates without As(III) before observation.

Quantitation of FND Uptake. The worms fed with FNDs were digested in 1:1 (v/v) mixtures of 65% $HClO_4$ and 30% H_2O_2 at 100 °C in a 100 W microwave reactor (Discover BenchMate, CEM) for 30 min, followed by treatment in concentrated HNO_3 and 30% H_2O_2 at 100 °C for 30 min.[23] After complete digestion of the specimens, FNDs were gathered by centrifugation. Fluorescence spectra of FNDs dispersed in water were acquired with a home-built spectrometer detailed in refs 11 and 42. The amounts of FNDs collected were calculated from the fluorescence intensity measurements at 685 nm according to a standard calibration curve, obtained by plotting the fluorescence intensity of the material against its concentration gradient.

Acknowledgment. We thank K. Blackwell at Harvard Medical School and the *Caenorhabditis* Genetic Center (CGC), supported by a grant from the NIH, for providing *gcs-1::gfp* and *daf-16::gfp* transgenic strains, respectively. We also thank V. H.-C. Liao at National Taiwan University for helpful discussion and technical assistance. This work is supported by Academia Sinica and the National Science Council, Taiwan, with Grant No. 98-2120-M-001-001.

Supporting Information Available. Figures and a video of *C. elegans* fed with FNDs. This material is available free of charge via the Internet at http://pubs.acs.org.

REFERENCES AND NOTES

(1) Sharma, P.; Brown, S.; Walter, G.; Santra, S.; Moudgil, B. *Adv. Colloid Interface Sci.* **2006**, *123−126*, 471–485.

DOI: 10.1021/nl1021909 | *Nano Lett.* **XXXX,** *xxx,* 000–000

(2) Gao, X.; Cui, Y.; Levenson, R. M.; Chung, L. W.; Nie, S. *Nat. Biotechnol.* **2004**, *22*, 969–976.
(3) Lim, S. F.; Riehn, R.; Ryu, W. S.; Khanarian, N.; Tung, C. K.; Tank, D.; Austin, R. H. *Nano Lett.* **2006**, *6*, 169–174.
(4) Park, J. H.; Gu, L.; von Maltzahn, G.; Ruoslahti, E.; Bhatia, S. N.; Sailor, M. J. *Nat. Mater.* **2009**, *8*, 331–336.
(5) Yang, S. T.; Cao, L.; Luo, P. G.; Lu, F.; Wang, X.; Wang, H.; Meziani, M. J.; Liu, Y.; Qi, G.; Sun, Y. P. *J. Am. Chem. Soc.* **2009**, *131*, 11308–11309.
(6) Welsher, K.; Liu, Z.; Sherlock, S. P.; Robinson, J. T.; Chen, Z.; Daranciang, D.; Dai, H. *Nat. Nanotechnol.* **2009**, *4*, 773–780.
(7) Yu, S.-J.; Kang, M.-W.; Chang, H.-C.; Chen, K.-M.; Yu, Y.-C. *J. Am. Chem. Soc.* **2005**, *127*, 17604–17605.
(8) Fu, C.-C.; Lee, H.-Y.; Chen, K.; Lim, T.-S.; Wu, H.-Y.; Lin, P.-K.; Wei, P.-K.; Tsao, P.-H.; Chang, H.-C.; Fann, W. *Proc. Natl. Acad. Sci. U.S.A.* **2007**, *104*, 727–732.
(9) Neugart, F.; Zappe, A.; Jelezko, F.; Tietz, C.; Boudou, J.-P.; Krueger, A.; Wrachtrup, J. *Nano Lett.* **2007**, *7*, 3588–3591.
(10) Faklaris, O.; Garrot, D.; Joshi, V.; Druon, F.; Boudou, J.-P.; Sauvage, T.; Georges, P.; Curmi, P. A.; Treussart, F. *Small* **2008**, *4*, 2236–2239.
(11) Chang, Y.-R.; Lee, H.-Y.; Chen, K.; Chang, C.-C.; Tsai, D.-S.; Fu, C.-C.; Lim, T.-S.; Tzeng, Y.-K.; Fang, C.-Y.; Han, C.-C.; Chang, H.-C.; Fann, W. *Nat. Nanotechnol.* **2008**, *3*, 284–288.
(12) Mohan, N.; Tzeng, Y.-K.; Yang, L.; Chen, Y.-Y.; Hui, Y. Y.; Fang, C.-Y.; Chang, H.-C. *Adv. Mater.* **2010**, *22*, 843–847.
(13) Liu, K.-K.; Cheng, C.-L.; Chang, C.-C.; Chao, J.-I. *Nanotechnology* **2007**, *18*, 325102.
(14) Schrand, A. M.; Huang, H.; Carlson, C.; Schlager, J.; Osawa, E.; Hussain, S.; Dai, L. *J. Phys. Chem. B* **2007**, *111*, 2–7.
(15) Vial, S.; Mansuy, C.; Sagan, S.; Irinopoulou, T.; Burlina, F.; Boudou, J.-P.; Chassaing, G.; Lavielle, S. *ChemBioChem* **2008**, *9*, 2113–2119.
(16) Vaijayanthimala, V.; Tzeng, Y.-K.; Chang, H.-C.; Li, C. L. *Nanotechnology* **2009**, *20*, 425103.
(17) Faklaris, O.; Joshi, V.; Irinopoulou, T.; Tauc, P.; Sennour, M.; Girard, H.; Gesset, C.; Arnault, J. C.; Thorel, A.; Boudou, J.-P.; Curmi, P. A.; Treussart, F. *ACS Nano* **2009**, *3*, 3955–3962.
(18) Sulston, J. E.; Horvitz, H. R. *Dev. Biol.* **1977**, *56*, 110–156.
(19) Sulston, J. E.; Schierenberg, E.; White, J. G.; Thomson, J. N. *Dev. Biol.* **1983**, *100*, 64–119.
(20) The C. elegans Sequencing Consortium et al. *Science* **1998**, *282*, 2012−2018.
(21) Anderson, G. L.; Boyd, W. A.; Williams, P. L. *Environ. Toxicol. Chem.* **2001**, *20*, 833–838.
(22) Dhawan, R.; Dusenbery, D. B.; Williams, P. L. *J. Toxicol. Environ. Health, Part A* **1999**, *58*, 451–462.
(23) Yuan, Y.; Chen, Y.; Liu, J. H.; Wang, H.; Liu, Y. *Diamond Relat. Mater.* **2009**, *18*, 95–100.
(24) Yuan, Y.; Wang, X.; Jia, G.; Liu, J. H.; Wang, T.; Gu, Y.; Yang, S. T.; Zhen, S.; Wang, H.; Liu, Y. *Diamond Relat. Mater.* **2009**, *18*, 291–299.
(25) Lim, S. F.; Riehn, R.; Ryu, W. S.; Khanarian, N.; Tung, C. K.; Tank, D.; Austin, R. H. *Nanotechnology* **2009**, *20*, 405701.
(26) Roh, J. Y.; Sim, S. J.; Yi, J.; Park, K.; Chung, K. H.; Ryu, D. Y.; Choi, J. *Environ. Sci. Technol.* **2009**, *43*, 3933–3940.
(27) Pluskota, A.; Horzowski, E.; Bossinger, O.; von Mikecz, A. *PLoS ONE* **2009**, *4*, No. e6622.
(28) McGhee, J. D. *The C. elegans Intestine, WormBook*; The *C. elegans* Research Community, DOI 10.1895/wormbook.1.133.1, March 27, 2007.
(29) Huang, L.-C.; Chang, H.-C. *Langmuir* **2004**, *20*, 5879–5884.
(30) Dahoumane, S. A.; Nguyen, M. N.; Thorel, A.; Boudou, J.-P.; Chehimi, M. M.; Mangeney, C. *Langmuir* **2009**, *25*, 9633–9638.
(31) Karp, G. *Cell & Molecular Biology*, 2nd ed.; Wiley; New York, 1999).
(32) Mello, C. C.; Kramer, J. M.; Stinchcomb, D.; Ambros, V. *EMBO J.* **1991**, *10*, 3959–3970.
(33) Wolke, U.; Jezuit, E. A.; Priess, J. R. *Development* **2007**, *134*, 2227–2236.
(34) Ralser, M.; Benjamin, I. J. *BMC Res. Notes* **2008**, *1*, 19.
(35) Hekimi, S.; Burgess, J.; Bussière, F.; Meng, Y.; Bénard, C. *Trends Genetics* **2001**, *17*, 712–718.
(36) Kim, J.; Takahashi, M.; Shimizu, T.; Shirasawa, T.; Kajita, M.; Kanayama, A.; Miyamoto, Y. *Mech. Ageing Dev.* **2008**, *129*, 322–331.
(37) Greenwald, I. *Introduction to Signal Transduction, WormBook*; The C. elegans Research Community, DOI 10.1895/wormbook.1.20.1, 2005.
(38) Huang, H.; Tindall, D. J. *J. Cell Sci.* **2007**, *120*, 2479–2487.
(39) Baumeister, R.; Schaffitzel, E.; Hertweck, M. *J. Endocrinol.* **2006**, *190*, 191–202.
(40) Henderson, S. T.; Johnson, T. E. *Curr. Biol.* **2001**, *11*, 1975–1980.
(41) An, J. H.; Blackwell, T. K. *Genes Dev.* **2003**, *17*, 1882–1893.
(42) Wee, T.-L.; Mau, Y.-W.; Fang, C.-Y.; Hsu, H.-L.; Han, C.-C.; Chang, H.-C. *Diamond Relat. Mater.* **2009**, *18*, 567–573.
(43) Brenner, S. *Genetics* **1974**, *77*, 71–94.
(44) Liao, V. H.; Yu, C. W. *Biometals* **2005**, *18*, 519–528.

DOI: 10.1021/nl1021909 | *Nano Lett.* **XXXX,** *xxx,* 000–000